Supporting Information

Metallic mesoporous oxide single crystals delivering enhanced electrocatalytic performance

Menghui Han,[abcd] Fangyuan Cheng*[abcd] and Kui Xie*[abcde]

[a] College of Chemistry and Materials Science, Fujian Normal University, Fuzhou 350117, China.

[b] Key Laboratory of Design & Assembly of Functional Nanostructures, Fujian Institute of Research on the Structure of Matter, Chinese Academy of Sciences, Fuzhou, Fujian 350002, China.

[c] Fujian Science & Technology Innovation Laboratory for Optoelectronic Information of China, Fuzhou, Fujian 350108, China.

[d] Fujian College, University of Chinese Academy of Sciences, Fuzhou 350108, China.

[e] School of Mechanical Engineering, Shanghai Jiao Tong University, 800 Dongchuan Road, Shanghai, 200240, China.

* Corresponding author: cfy@fjirsm.ac.cn (F. Cheng), xiekui@sjtu.edu.cn (K. Xie).

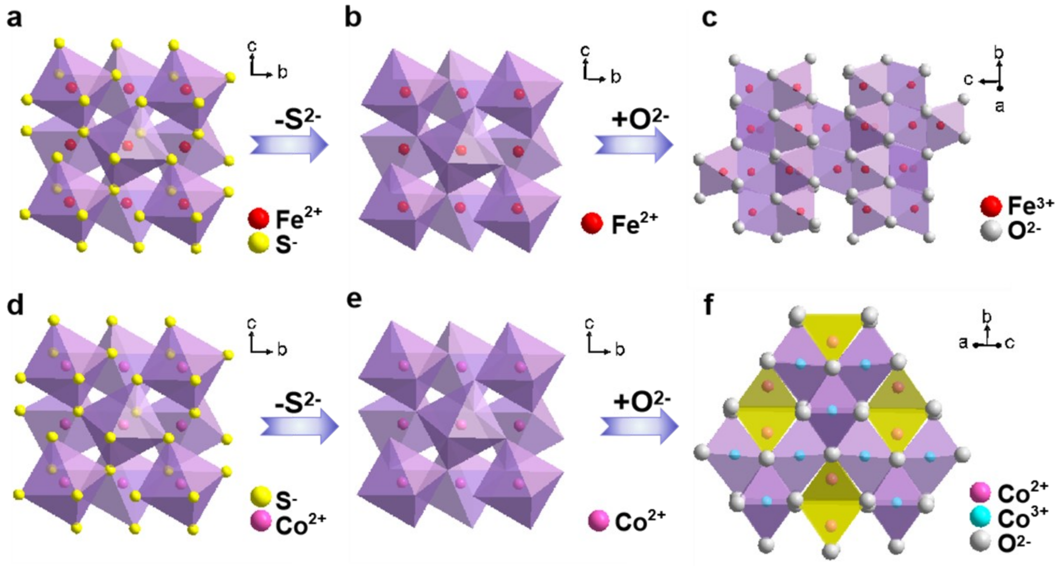

Fig. S1 Growth mechanism of PSC Fe_2O_3 and PSC Co_3O_4.

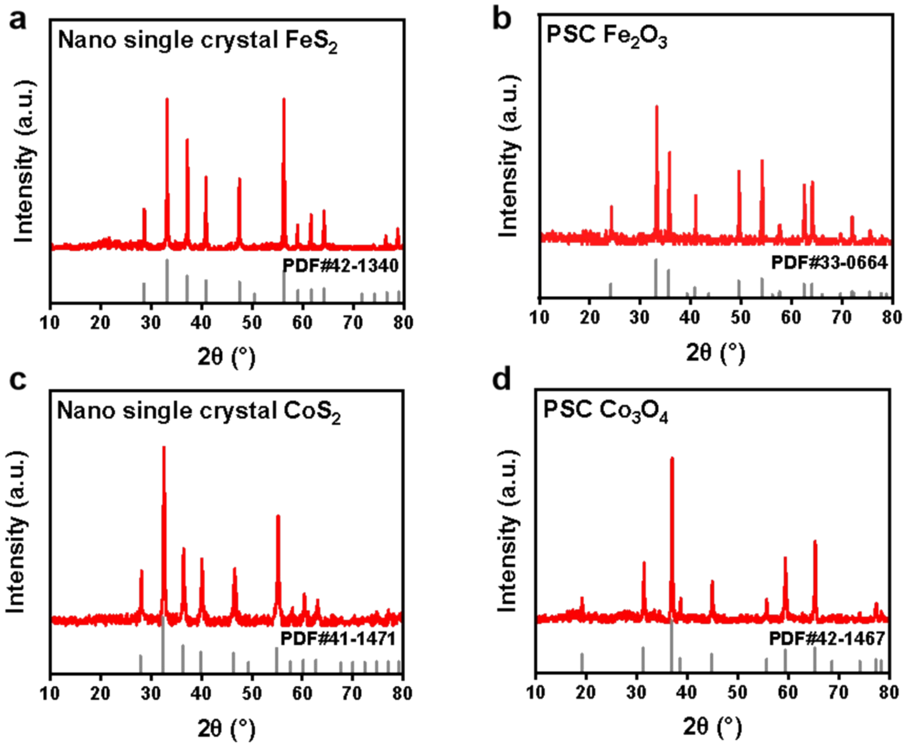

Fig. S2 XRD patterns of different nano single crystals compared with standard cards. (a) FeS_2 nano single crystal. (b) PSC Fe_2O_3. (c) CoS_2 nano single crystal. (d) PSC Co_3O_4.

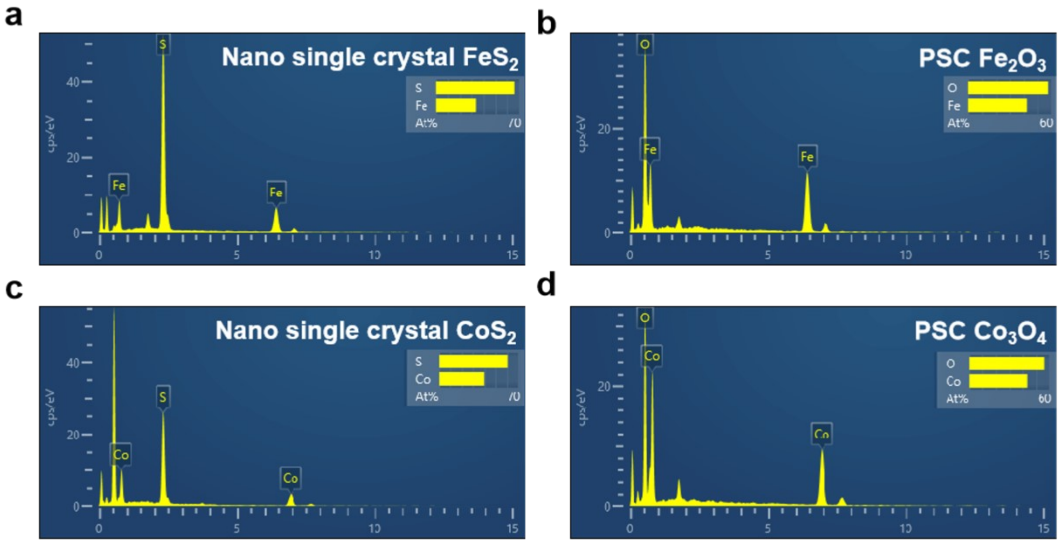

Fig. S3 EDS images. (a) Precursor FeS_2 nano single crystal. (b) PSC Fe_2O_3. (c) Precursor CoS_2 nano single crystal. (d) PSC Co_3O_4.

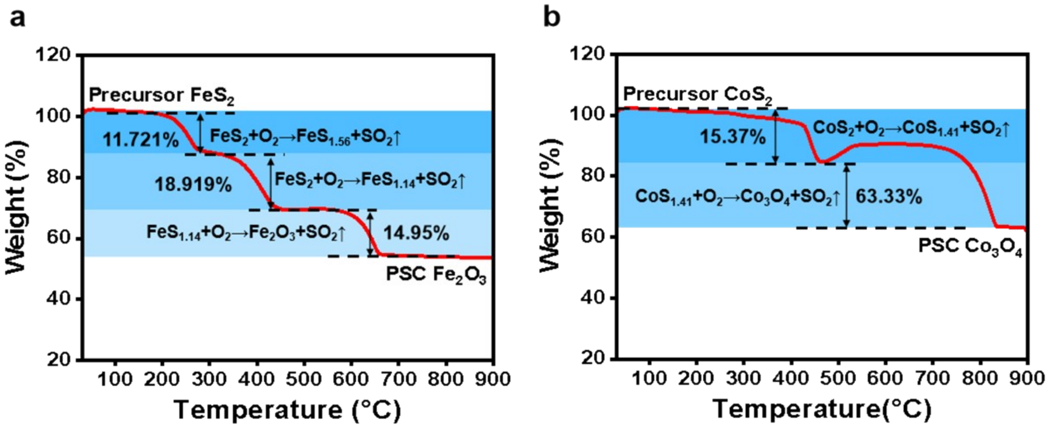

Fig. S4 TGA curves under the air atmosphere. (a) From precursor FeS_2 to PSC Fe_2O_3. (b) From precursor CoS_2 to PSC Co_3O_4.

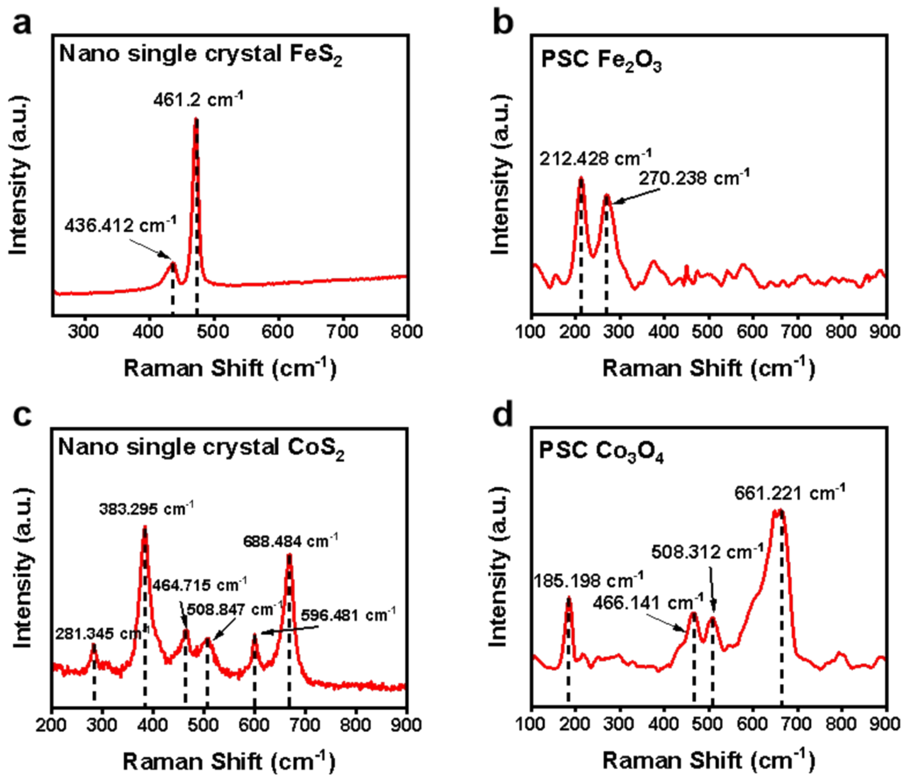

Fig. S5 Raman spectras. (a) FeS_2 nano single crystal. (b) PSC Fe_2O_3. (c) CoS_2 nano single crystal. (d) PSC Co_3O_4.

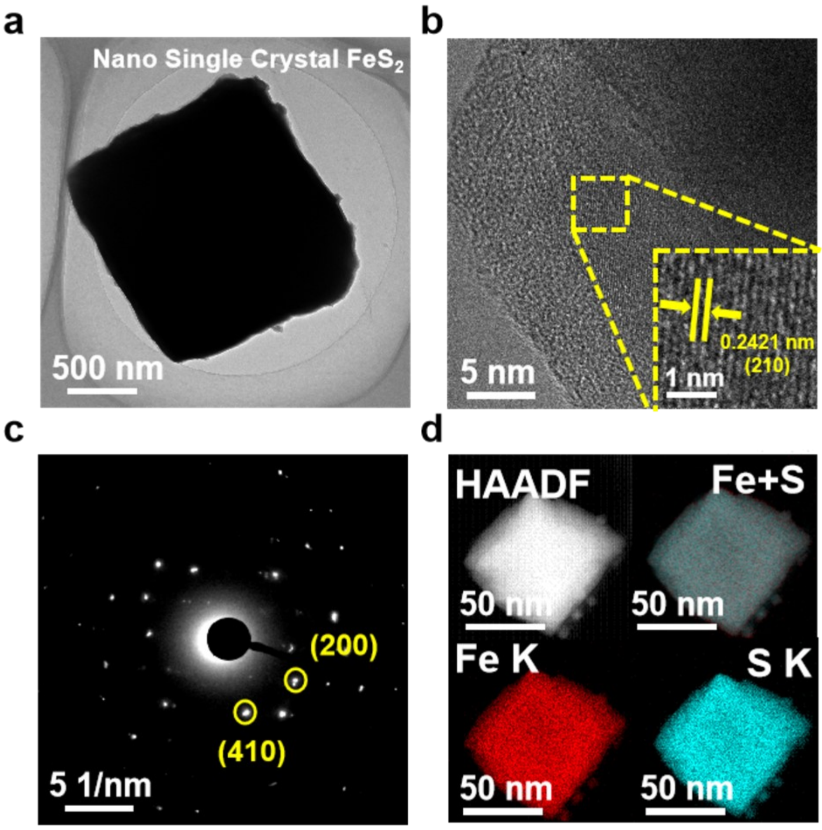

Fig. S6 (a) FETEM image of precursor FeS_2 nano single crystal. (b) HRTEM image of precursor FeS_2 nano single crystal. (c) SAED pattern of precursor FeS_2 nano single crystal. (d) EDS elemental mapping results of precursor FeS_2 nano single crystal.

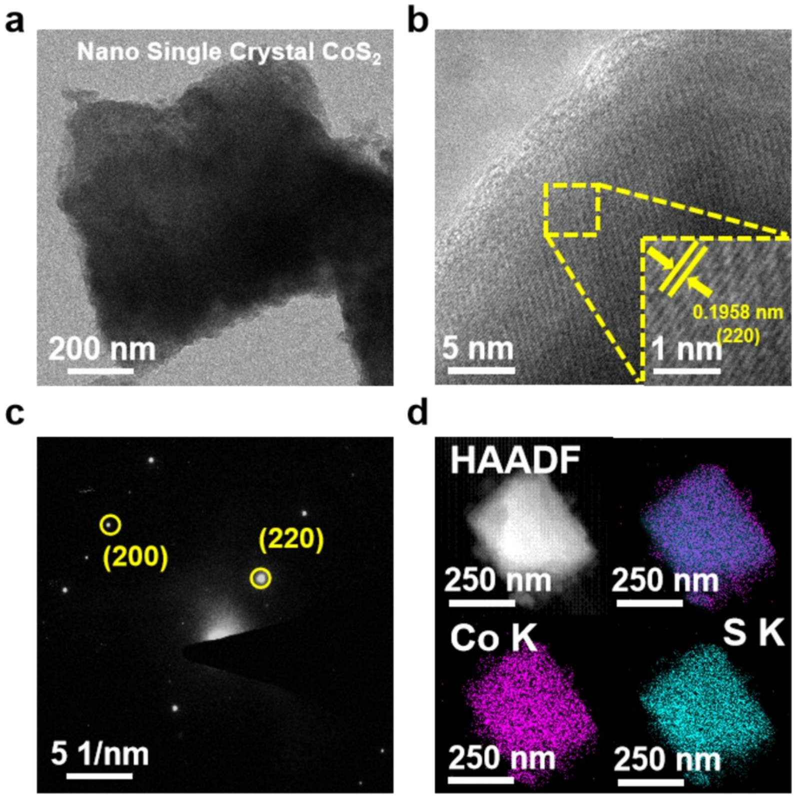

Fig. S7 (a) FETEM image of precursor CoS_2 nano single crystal. (b) HRTEM image of precursor CoS_2 nano single crystal. (c) SAED pattern of precursor CoS_2 nano single crystal. (d) EDS elemental mapping results of precursor CoS_2 nano single crystal.

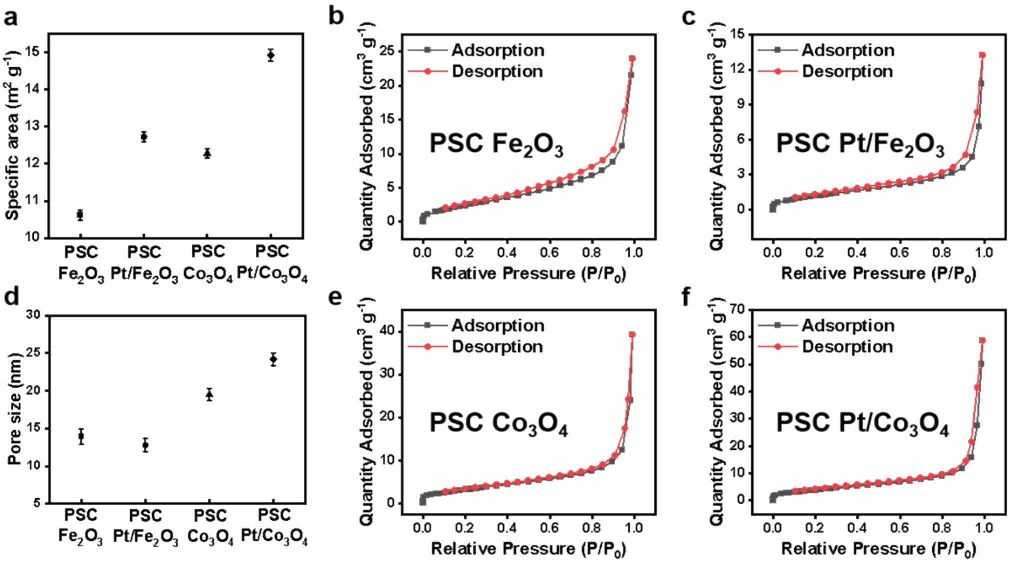

Fig. S8 Specific area, pore size, and N_2 absorption-desorption isotherm of PSC Fe_2O_3, PSC Co_3O_4, Pt/Fe_2O_3 and Pt/Co_3O_4. (a) Specific area. (b-c) N_2 absorption-deorption isotherm, (b) PSC Fe_2O_3, (c) PSC Pt/Co_3O_4. (d) Pore size. (e-f) N_2 absorption-deorption isotherm, (e) PSC Pt/Fe_2O_3, (f) PSC Co_3O_4.

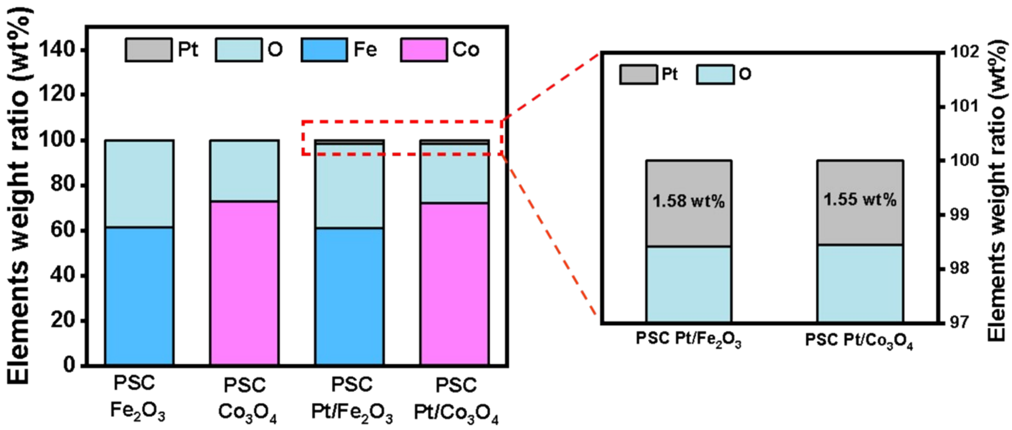

Fig. S9 Weight content ratio of each element in PSC Fe_2O_3, PSC Co_3O_4, Pt/Fe_2O_3 and Pt/Co_3O_4.

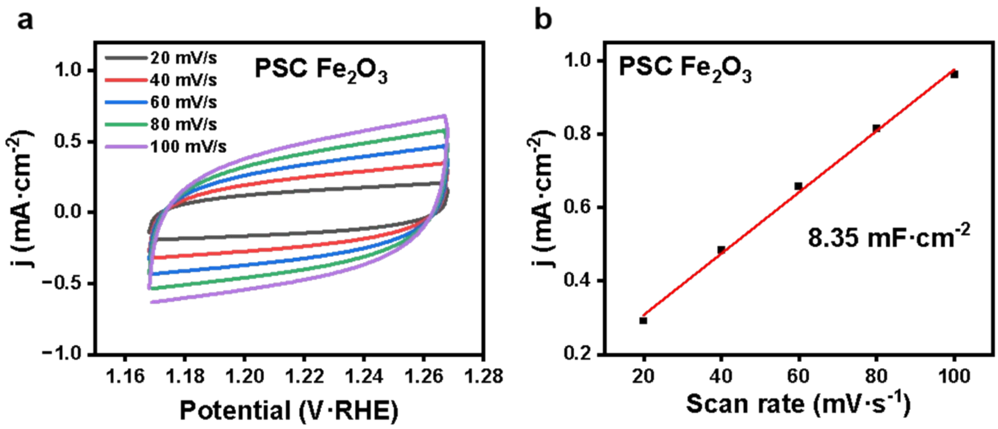

Fig. S10 PSC Fe_2O_3 of (a) CV curves. (b) Linear relationship between current density and scan rate.

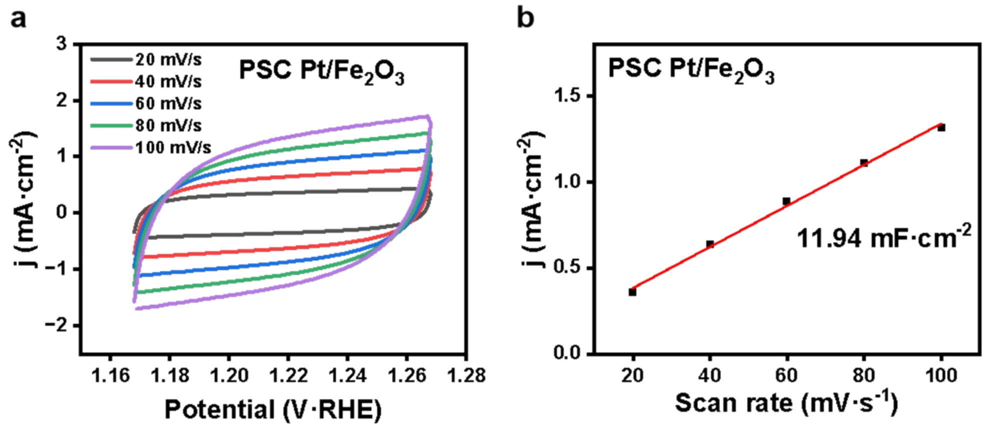

Fig. S11 PSC Pt/Fe_2O_3 of (a) CV curves. (b) Linear relationship between current density and scan rate.

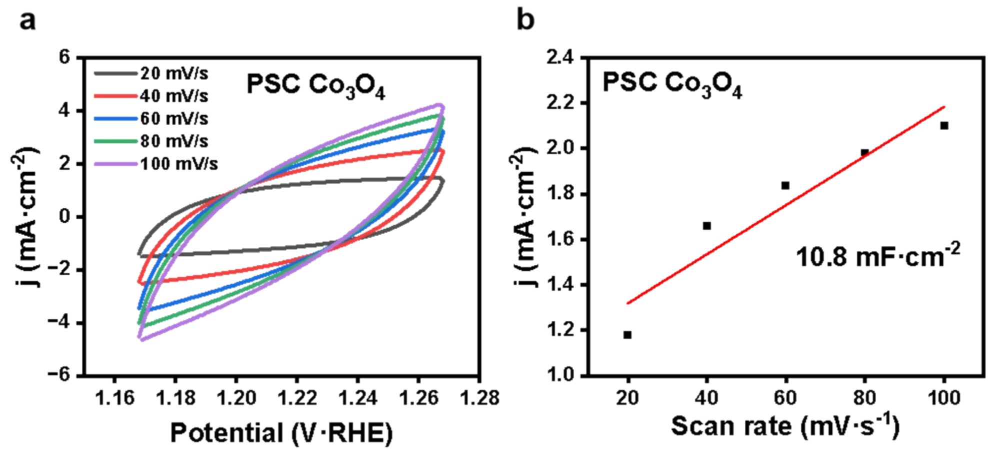

Fig. S12 PSC Co_3O_4 of (a) CV curves. (b) Linear relationship between current density and scan rate.

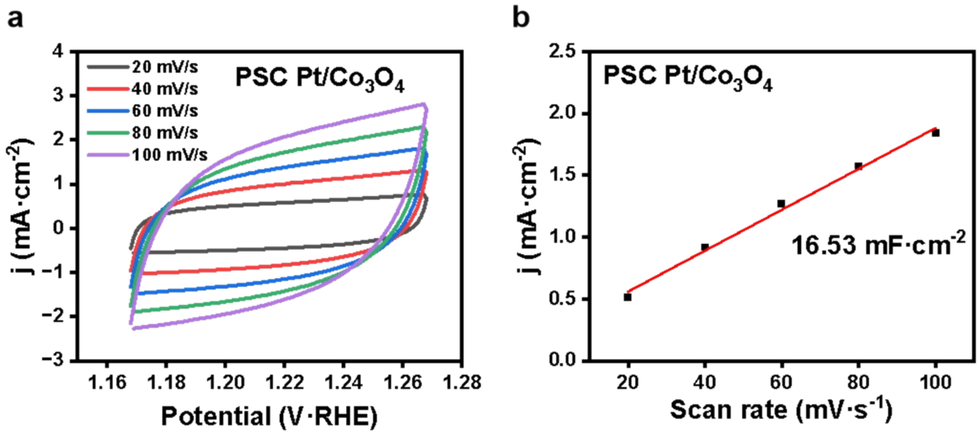

Fig. S13 PSC Pt/Co_3O_4 of (a) CV curves. (b) Linear relationship between current density and scan rate.

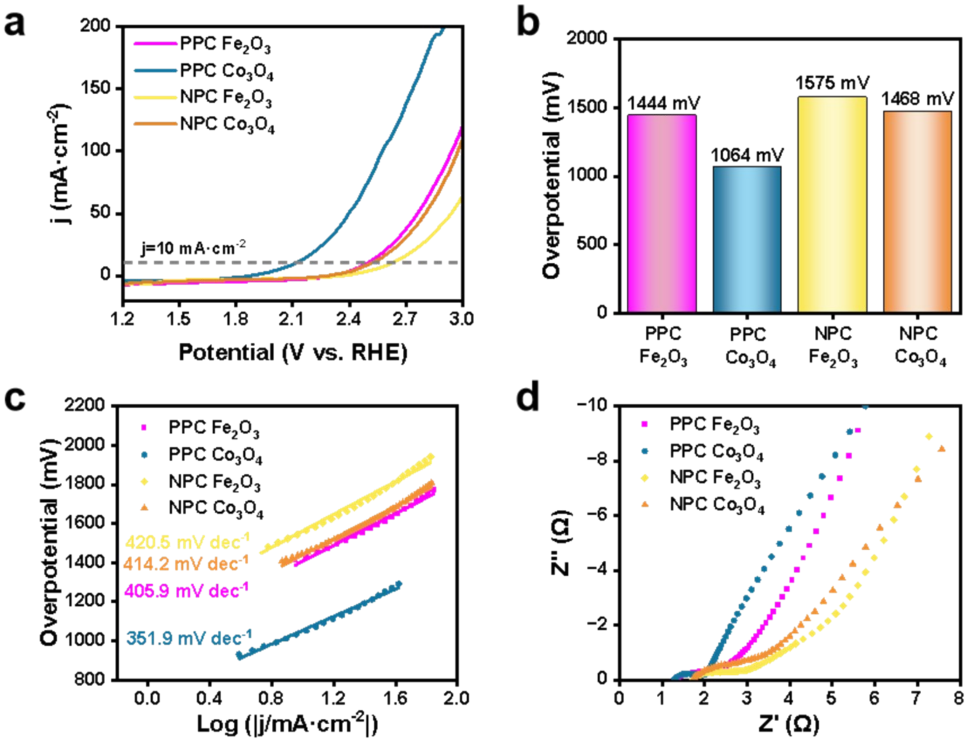

Fig. S14 The OER electrocatalytic performance of PPC Fe_2O_3, NPC Fe_2O_3, PPC Co_3O_4, NPC Co_3O_4 in 1M KOH solution. (a) LSV curves. (b) Overpotentials at 10 mA cm^{-2}. (c) Tafel slopes. (d) EIS curves.

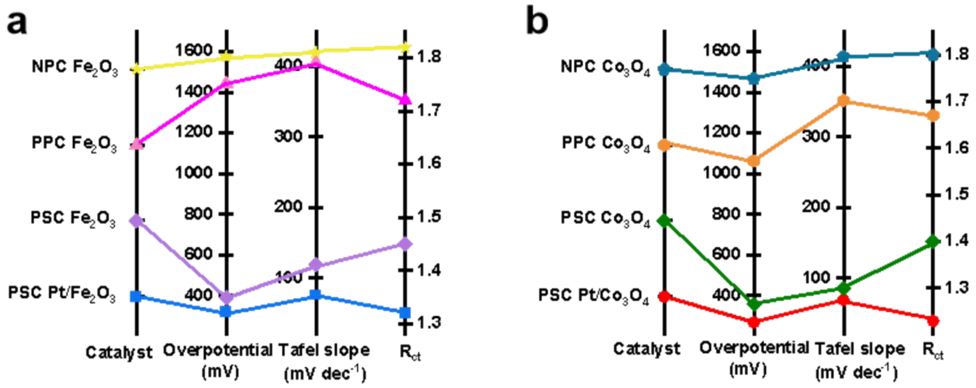

Fig. S15 Comparisons of PSCs, PPC, NPC catalysts in overpotential, tafel slope and R_{ct}. (a) Fe_2O_3 catalysts. (b) Co_3O_4 catalysts.

Table S1. The Summary of the performance of different catalysts for OER.

Catalysts	Electrolyte	η (mV) at j=10 mA·cm^{-2}	Tafel slope (mV·dec^{-1})	References
Fe_2O_3-(012)NCs	1 M KOH	317	59	[1]
Fe_2O_3 @Mo	1 M KOH	359	80	[2]
$NiFeO_x$	1 M KOH	380	/	[3]
Fe_2O_3/FeS	1 M KOH	320	90	[4]
$CoFe_2O_4$	1 M KOH	320	71	[5]
Co_3O_4@CoO SC	0.5 M KOH	430	60	[6]
Co_3O_4/SnO_2	1 M KOH	487	100	[7]
C-Co/Co_3O_4	1 M KOH	352	80	[8]
Ce-Co_3O_4	0.5 M H_2SO_4	345	85.15	[9]
PtFe/G-2h	1 M KOH	315	56	[10]
O–MoS_2@Pt	1 M KOH	244	53	[11]
Pt@$Ti_3C_2T_x$–rGO 3 : 1	0.1 M $HClO_4$	490	165.3	[12]
1%Pt-substituted-Co_3O_4	1 M KOH	380	117	[13]
RuO_2/$(Co,Mn)_3O_4$/CC	0.5 M H_2SO_4	270	77	[14]
Fe_2O_3 sphere	1 M KOH	396	128	[2]
Co_3O_4 nano spheres	1 M KOH	407	107	[7]
PSC Fe_2O_3	1 M KOH	391	119	This work
PSC Co_3O_4	1 M KOH	360	86	This work
PSC Pt/Fe_2O_3	1 M KOH	319	76	This work
PSC Pt/Co_3O_4	1 M KOH	269	69	This work

Reference

1 H. Wu, T. Yang, Y. Du, L. Shen and G. W. Ho, *Adv. Mater.*, 2018, **30**, 1804341.

2 A. Maurya and M. Yadav, *J. Alloy. Compd.*, 2023, **956**, 170208.

3 W. Moschkowitsch, N. Zion, H. C. Honig, N. Levy, D. A. Cullen and L. Elbaz, *ACS Catal.*, 2022, **12**, 12162-12169.

4 N. A. Khan, N. Rashid, I. Ahmad, Zahidullah, R. Zairov, H. u. Rehman, M. F. Nazar and U. Jabeen, *Int. J. Hydrog. Energy*, 2022, **47**, 22340-22347.

5 F. Waag, B. Gökce, C. Kalapu, G. Bendt, S. Salamon, J. Landers, U. Hagemann, M. Heidelmann, S. Schulz, H. Wende, N. Hartmann, M. Behrens and S. Barcikowski, *Sci Rep*, 2017, **7**, 13161.

6 C.-W. Tung, Y.-Y. Hsu, Y.-P. Shen, Y. Zheng, T.-S. Chan, H.-S. Sheu, Y.-C. Cheng and H. M. Chen, *Nat. Commun.*, 2015, **6**, 8106.

7 J. Milikić, S. Knežević, M. Ognjanović, D. Stanković, L. Rakočević and B. Šljukić, *Int. J. Hydrog. Energy*, 2023, **48**, 27568-27581.

8 L. Hang, Y. Sun, D. Men, S. Liu, Q. Zhao, W. Cai and Y. Li, *J. Mater. Chem. A*, 2017, **5**, 11163-11170.

9 J. Yang, F. Xu, W. Zhao, L. Liu and B. Weng, *Small*, 2024, **20**, 2309363.

10 H. Xiao, X. Yang, M. Zhao, R. Zhang, Y. Jing, L. Zhang, Y. He, H. Wu and J. Jia, *Int. J. Hydrog. Energy*, 2023, **48**, 38728-38741.

11 F. Gong, S. Ye, M. Liu, J. Zhang, L. Gong, G. Zeng, E. Meng, P. Su, K. Xie, Y. Zhang and J. Liu, *Nano Energy*, 2020, **78**, 105284.

12 L. Vazhayal, S. B. Alex and S. K. Haram, *J. Mater. Chem. A*, 2024, **12**, 27671-27685.

13 S. Nellaiappan, N. Jhariya, S. Irusta and A. Singhal, *Electrochim. Acta*, 2021, **365**, 137234.

14 S. Niu, X.-P. Kong, S. Li, Y. Zhang, J. Wu, W. Zhao and P. Xu, *Appl. Catal. B-Environ.*, 2021, **297**, 120442.